
Spectral density of the non-backtracking operator

A. SAADE¹, F. KRZAKALA^{1,2} and L. ZDEBOROVÁ³

¹ *Laboratoire de Physique Statistique, CNRS UMR 8550, Université P. et M. Curie Paris 6 et École Normale Supérieure, 24, rue Lhomond, 75005 Paris, France.*

² *ESPCI and CNRS UMR 7083 Gulliver, 10 rue Vauquelin, Paris 75005 France*

³ *Institut de Physique Théorique, IPhT, CEA Saclay and URA 2306, CNRS - Orme des Merisiers 91191 Gif-sur-Yvette, France.*

PACS 89.20.-a – Interdisciplinary applications of physics
PACS 89.75.Hc – Networks and genealogical trees
PACS 02.10.Yn – Matrix theory

Abstract –The non-backtracking operator was recently shown to provide a significant improvement when used for spectral clustering of sparse networks. In this paper we analyze its spectral density on large random sparse graphs using a mapping to the correlation functions of a certain interacting quantum disordered system on the graph. On sparse, tree-like graphs, this can be solved efficiently by the cavity method and a belief propagation algorithm. We show that there exists a paramagnetic phase, leading to zero spectral density, that is stable outside a circle of radius $\sqrt{\rho}$, where ρ is the leading eigenvalue of the non-backtracking operator. We observe a second-order phase transition at the edge of this circle, between a zero and a non-zero spectral density. The fact that this phase transition is absent in the spectral density of other matrices commonly used for spectral clustering provides a physical justification of the performances of the non-backtracking operator in spectral clustering.

Introduction. – Clustering and community detection are central tasks in the study of social, biological, and technological networks. Sparse networks, where the average degree of every node is a constant independent on the size of the network, are arguably the most relevant for applications, and at the same time the most challenging for clustering. Spectral methods are among the most widely used for this task. They are conceptually simply based on the computation of principal eigenvalues and eigenvectors of an operator associated with the network [1]. Most commonly this operator is the adjacency matrix, the Laplacian (symmetrized and/or normalized), the random walk matrix, or the modularity matrix. The spectrum of these matrices generically decomposes into a bulk of non-informative eigenvalues, and some informative eigenvalues separated from the bulk by a gap. The eigenvectors corresponding to the informative eigenvalues are correlated with the cluster structure. However, on sparse networks, spectral clustering based on these commonly used matrices does not perform as well as for instance methods based on Bayesian inference that can perform well even when the tails of the bulk of the spectrum flood the informative eigenvalue [2].

Recently, the author of [3] proposed the so-called non-backtracking operator for spectral clustering and conjectured that this method is optimal: it is able to find clusters for large random clustered networks (in the stochastic block model) as long as it is information theoretically possible. The non-backtracking matrix B , associated with an undirected graph, encodes adjacency between directed edges. Its element $B_{i \rightarrow j, k \rightarrow l}$ is one if the edge $i \rightarrow j$ flows into the edge $k \rightarrow l$, i.e. $j = k$ and $i \neq l$, and zero otherwise. The authors of [3] give theoretical and numerical evidence that apart from the informative eigenvalues the spectrum of this matrix is confined to the circle of radius the square root of the average excess degree of the network, not presenting the so-called Lifshitz tails [2] that spoil the performance of spectral clustering for the other matrices mentioned above.

In order to understand better the performance of spectral clustering it is crucial to understand in detail the spectral properties of the associated operators on random graphs. Analytical results for spectral densities of sparse random graphs are largely based on the method of replicas and cavity and were mostly developed and studied for symmetric random matrices [4–8]. The result most rele-

vant to the present work is that the tails of the spectrum of the commonly studied matrices associated with random graphs (for concreteness consider Erdős-Rényi graphs) are extended, see e.g. [2, 6, 7]. On the other hand the result of [3] suggest that the spectrum of the non-backtracking operator has no such tails.

Here, we derive the spectral density of the non-backtracking operator for random locally tree-like graphs in the limit of large size. We use the methods of [4, 5, 7, 8] based on expressing the spectral density as the internal energy of a disordered system with quenched disorder. In particular we use the method applied to non-symmetric matrices as developed in [9, 10]. The corresponding disordered system is then studied using the cavity method and the associated belief propagation (BP) algorithm [11].

Our main result is the discovery of a phase transition in the disordered system associated with the spectrum of the non-backtracking operator which translates to the fact that the spectral density can be different from zero only inside a circle of radius equal to the square root of the leading eigenvalue. This is fundamentally different from the spectral properties of the commonly considered operators associated with a sparse random graph where the tails of the spectrum are unbounded in the limit of large size. The presence of this phase transition provides a physics-based explanation of the superior performance of the non-backtracking-based spectral clustering from [3].

Statistical physics formulation. – To tackle the problem, following the method of [9], we map the computation of the spectral density to a problem of statistical physics of disordered systems. It has been shown [12–14] that all the eigenvalues λ_i of B that are different from ± 1 are the roots of the polynomial

$$\det [D - zA - (1 - z^2)\mathbf{1}] = \prod_i^{2N} (z - \lambda_i). \quad (1)$$

This is known in graph theory as the Ihara-Bass formula. We define the spectral density at $z \in \mathbb{C}$ as

$$\nu(z) = \frac{1}{2N} \sum_{i=1}^{2N} \delta(z - \lambda_i). \quad (2)$$

Using the complex representation of the Dirac delta

$$\delta(z - \mu) = \frac{1}{\pi} \partial_{\bar{z}} (z - \mu)^{-1}, \quad (3)$$

where $\partial_{\bar{z}}$ is the Wirtinger derivative, one can show that

$$\nu(z) = \frac{1}{2\pi N} \partial_{\bar{z}} \partial_z \log \det ((D - zA - (1 - z^2)\mathbf{1})^\dagger) \quad (4)$$

$$\times (D - zA - (1 - z^2)\mathbf{1}) \quad (5)$$

whenever z is not an eigenvalue of B . To make this formula valid for all $z \in \mathbb{C}$, we add an infinitesimal regularizer $\epsilon^2 \mathbf{1}$ in the determinant, so that one can rewrite

$$\nu(z) = \lim_{\epsilon \rightarrow 0} \frac{1}{2\pi N} \partial_{\bar{z}} \partial_z \log \det \mathcal{M}_\epsilon \quad (6)$$

with

$$\mathcal{M}_\epsilon(z, A) = \begin{pmatrix} \epsilon \mathbf{1} & i(D - zA - (1 - z^2)\mathbf{1}) \\ i(D - zA - (1 - z^2)\mathbf{1})^\dagger & \epsilon \mathbf{1} \end{pmatrix}. \quad (7)$$

All the eigenvalues of this matrix have a positive real part ϵ , so we can use the complex Gaussian representation of the determinant

$$(\det \mathcal{M}_\epsilon)^{-1} = \left(\frac{1}{\pi}\right)^{2N} \int \prod_i^{2N} d\psi_i d\bar{\psi}_i e^{-\sum_{j,k} \bar{\psi}_j \mathcal{M}_{jk} \psi_k}. \quad (8)$$

To take advantage of the block structure of the kernel, we group the variables into pairs

$$\chi_i = \begin{pmatrix} \psi_i \\ \psi_{i+N} \end{pmatrix}, \quad \forall 1 \leq i \leq N. \quad (9)$$

Finally, the computation of the spectral density has been mapped to a statistical physics problem

$$\nu(z) = -\lim_{\epsilon \rightarrow 0} \frac{1}{2\pi N} \partial_{\bar{z}} \partial_z \log \mathcal{Z}_\epsilon, \quad (10)$$

where the partition function

$$\mathcal{Z}_\epsilon = \int d\chi d\bar{\chi} e^{-\mathcal{H}} \quad (11)$$

corresponds to the Hamiltonian

$$\begin{aligned} \mathcal{H}_\epsilon = & \sum_{i=1}^N \chi_i^\dagger \begin{pmatrix} \epsilon & id_i - i(1 - z^2) \\ id_i - i(1 - \bar{z}^2) & \epsilon \end{pmatrix} \chi_i \\ & + i \sum_{i,j} \chi_i^\dagger \begin{pmatrix} 0 & -zA_{ij} \\ -\bar{z}A_{ij} & 0 \end{pmatrix} \chi_j. \end{aligned} \quad (12)$$

While the "Boltzmann weight" $e^{-\mathcal{H}_\epsilon}/\mathcal{Z}_\epsilon$ happens to be complex here, the algebraic analogy is enough to ensure that the cavity method still works out. Doing the derivative with respect to z , we can now express the spectral density in terms of one and two-points correlation functions, that can be computed using the cavity method

$$\nu(z) = \lim_{\epsilon \rightarrow 0} \frac{i}{\pi N} \partial_{\bar{z}} \left(z \sum_{i=1}^N \langle \chi_i^\dagger \sigma_+ \chi_i \rangle - \sum_{\langle i,j \rangle} \langle \chi_i^\dagger \sigma_+ \chi_j \rangle \right), \quad (13)$$

where the second sum is over pairs of neighbors and

$$\sigma_+ = \begin{pmatrix} 0 & 1 \\ 0 & 0 \end{pmatrix}. \quad (14)$$

The $\langle \rangle$ in (13) denotes averaging over the (complex) Boltzmann weight.

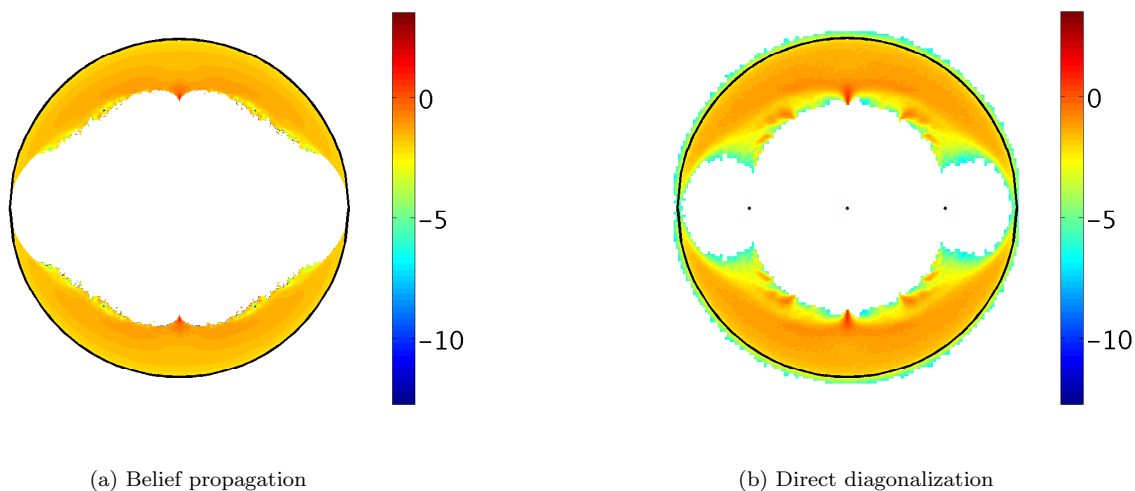


Fig. 1: Spectral density of the non-backtracking matrix in $\ln z$ -scale. Comparison between the result of belief propagation and direct diagonalization, on graphs of average degree $c = 3$. Figure (b) was obtained by diagonalizing 1000 matrices of size 3000×3000 . The black circle has radius \sqrt{c} . Figure (a) is the result of applying BP to a single graph of size 10000, at 600×600 different points $z \in \mathbb{C}$. The origins of the differences are discussed in the text.

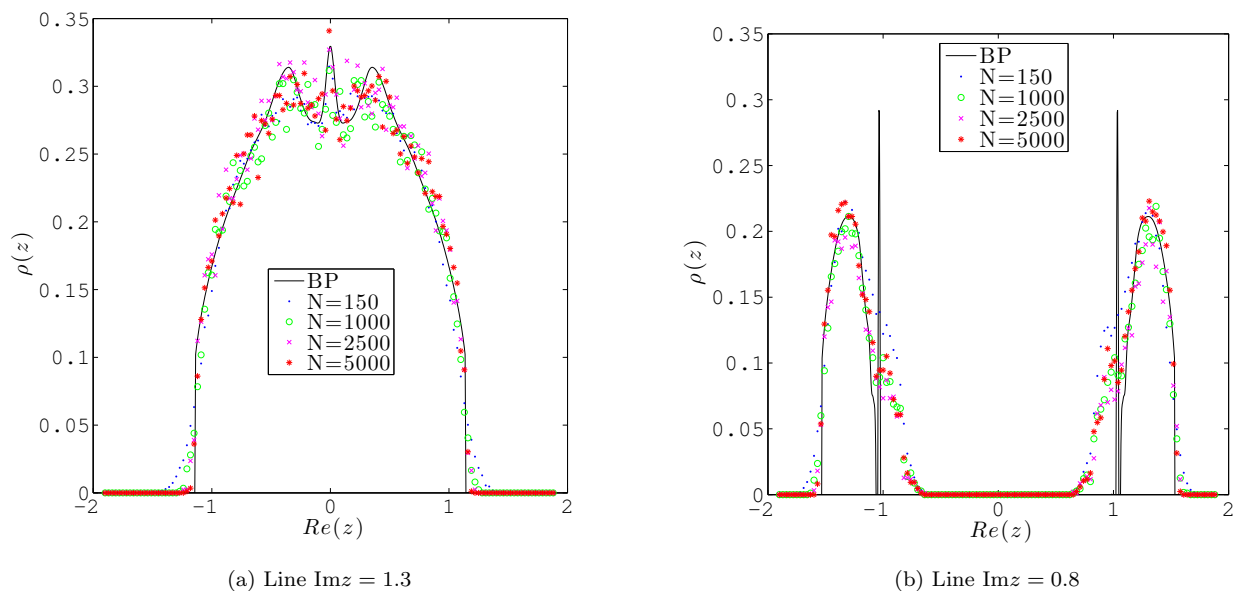


Fig. 2: Slices of the spectral density along two lines: comparison between BP (black line), and histograms of B 's eigenvalues corresponding to graphs of size N , and average connectivity $c = 3$. For each value of N represented, we diagonalized a number of random B matrices such that the total number of eigenvalues obtained is equal to 10^6 . We then extracted those close to the line represented in each subfigure. The location of the peaks on the right depends on the particular instance on the graph, as shown on figure 3.

The cavity method. – The Hamiltonian (12) corresponds to an effective quantum disordered spin system that can be written as

$$\mathcal{H}_\epsilon = \sum_{i=1}^N \mathcal{H}_i + \sum_{i<j \in \mathcal{G}} \mathcal{H}_{ij} \quad (15)$$

with

$$\mathcal{H}_i = \chi_i^\dagger \begin{pmatrix} \epsilon & id_i - i(1 - z^2) \\ id_i - i(1 - \bar{z}^2) & \epsilon \end{pmatrix} \chi_i \quad (16)$$

$$\mathcal{H}_{ij} = -i\chi_i^\dagger \begin{pmatrix} 0 & z \\ \bar{z} & 0 \end{pmatrix} \chi_j - i\chi_j^\dagger \begin{pmatrix} 0 & z \\ \bar{z} & 0 \end{pmatrix} \chi_i. \quad (17)$$

Denoting $P_{i \rightarrow j}(\chi_i)$ the distribution of the variable χ_i in the absence of node j , and $P_i(\chi_i)$ the actual marginal, the belief propagation recursion (exact on trees) reads [11]

$$P_{i \rightarrow j}(\chi_i) \propto e^{-\mathcal{H}_i} \int e^{-\sum_{l \in \partial i \setminus j} \mathcal{H}_{il}} \prod_{l \in \partial i \setminus j} P_{l \rightarrow i}(\chi_l) d\chi_l, \quad (18)$$

$$P_i(\chi_i) \propto e^{-\mathcal{H}_i} \int e^{-\sum_{l \in \partial i} \mathcal{H}_{il}} \prod_{l \in \partial i} P_{l \rightarrow i}(\chi_l) d\chi_l. \quad (19)$$

Because the Hamiltonian is quadratic, the variables χ_i are Gaussians of mean 0, and we can parametrize

$$P_{l \rightarrow i}(\chi_l) = \frac{1}{\pi^2 \det \Delta_{l \rightarrow i}} e^{-\chi_l^\dagger (\Delta_{l \rightarrow i})^{-1} \chi_l}, \quad (20)$$

$$P_i(\chi_i) = \frac{1}{\pi^2 \det \Delta_i} e^{-\chi_i^\dagger (\Delta_i)^{-1} \chi_i}. \quad (21)$$

Considerations of symmetry impose the following form for the matrices Δ

$$\Delta = \begin{pmatrix} a & i\bar{b} \\ i\bar{b} & a \end{pmatrix}, \quad (22)$$

where a is real and positive. Injecting this form in (18)-(19), we find

$$\frac{a_{i \rightarrow j}}{a_{i \rightarrow j}^2 + |b_{i \rightarrow j}|^2} = \epsilon + |z|^2 \sum_{l \in \partial i \setminus j} a_{l \rightarrow i}, \quad (23)$$

$$\frac{\bar{b}_{i \rightarrow j}}{a_{i \rightarrow j}^2 + |b_{i \rightarrow j}|^2} = (1 - d_i - z^2) - z^2 \sum_{l \in \partial i \setminus j} b_{l \rightarrow i}, \quad (24)$$

$$\frac{a_i}{a_i^2 + |b_i|^2} = \epsilon + |z|^2 \sum_{l \in \partial i} a_{l \rightarrow i}, \quad (25)$$

$$\frac{\bar{b}_i}{a_i^2 + |b_i|^2} = (1 - d_i - z^2) - z^2 \sum_{l \in \partial i} b_{l \rightarrow i}. \quad (26)$$

In the following, we take $\epsilon = 0$. It only remains to express the correlators (13) in terms of a and b . Then, from (19),

$$\langle \chi_i^\dagger \sigma_+ \chi_i \rangle = ib_i. \quad (27)$$

To express the second correlator we need the joint probability of χ_i and χ_j where i and j are neighbors:

$$P(\chi_i, \chi_j) \propto P_{j \rightarrow i}(\chi_j) P_{i \rightarrow j}(\chi_i) e^{-\mathcal{H}_{ij}}. \quad (28)$$

Some algebra then yields

$$\langle \chi_i^\dagger \sigma_+ \chi_j \rangle = i(-zb_{j \rightarrow i} b_i + \bar{z} a_{j \rightarrow i} a_i). \quad (29)$$

Replacing in (13) and using the BP recursions (23)-(26), the spectral density takes the form

$$\nu(z) = -\frac{1}{2\pi N z} \sum_{i=1}^N (1 - d_i + z^2) \partial_{\bar{z}} b_i. \quad (30)$$

To avoid numerical differentiation, we also compute the derivatives of these variables recursively

$$\partial_{\bar{z}} a_{i \rightarrow j} = -a_{i \rightarrow j} (a_{i \rightarrow j} A_{i \rightarrow j} - \bar{b}_{i \rightarrow j} B_{i \rightarrow j}) + b_{i \rightarrow j} (a_{i \rightarrow j} C_{i \rightarrow j} + \bar{b}_{i \rightarrow j} A_{i \rightarrow j}), \quad (31)$$

$$\partial_{\bar{z}} b_{i \rightarrow j} = -a_{i \rightarrow j} (b_{i \rightarrow j} A_{i \rightarrow j} + a_{i \rightarrow j} B_{i \rightarrow j}) - b_{i \rightarrow j} (-b_{i \rightarrow j} C_{i \rightarrow j} + a_{i \rightarrow j} A_{i \rightarrow j}), \quad (32)$$

$$\partial_{\bar{z}} \bar{b}_{i \rightarrow j} = -\bar{b}_{i \rightarrow j} (a_{i \rightarrow j} A_{i \rightarrow j} - \bar{b}_{i \rightarrow j} B_{i \rightarrow j}) - a_{i \rightarrow j} (a_{i \rightarrow j} C_{i \rightarrow j} + \bar{b}_{i \rightarrow j} A_{i \rightarrow j}), \quad (33)$$

where

$$A_{i \rightarrow j} = \sum_{l \in \partial i \setminus j} (z a_{l \rightarrow i} + |z|^2 \partial_{\bar{z}} a_{l \rightarrow i}), \quad (34)$$

$$B_{i \rightarrow j} = 2\bar{z} + \sum_{l \in \partial i \setminus j} (2z \bar{b}_{l \rightarrow i} + \bar{z}^2 \partial_{\bar{z}} \bar{b}_{l \rightarrow i}), \quad (35)$$

$$C_{i \rightarrow j} = z^2 \sum_{l \in \partial i \setminus j} \partial_{\bar{z}} b_{l \rightarrow i}. \quad (36)$$

and similar expressions for the derivatives of the "full" variables a_i and b_i in which $a_{i \rightarrow j}$ gets replaced by a_i in (31)-(33), and the sums in (34)-(36) become over all neighbors of i . Equations (23)-(24) and (31)-(36) are self-consistent BP equations which, when iterated, converge to a set of solutions $a_{i \rightarrow j}$, $b_{i \rightarrow j}$, $\partial_{\bar{z}} a_{i \rightarrow j}$, $\partial_{\bar{z}} b_{i \rightarrow j}$, $\partial_{\bar{z}} \bar{b}_{i \rightarrow j}$. We then compute the full variables a_i , b_i , $\partial_{\bar{z}} a_i$, $\partial_{\bar{z}} b_i$, $\partial_{\bar{z}} \bar{b}_i$ using equations (25)-(26) and the counterpart of equations (31)-(36) for the full variables. This finally allows us to compute the spectral density using expression (30).

The paramagnetic phase. – It is easy to see that the following assignment of the variables is a fixed point of the belief propagation equations

$$a_{i \rightarrow j} = 0 \quad \forall \langle i, j \rangle, \quad (37)$$

$$b_{i \rightarrow j} = -\frac{1}{z^2} \quad \forall \langle i, j \rangle \quad (38)$$

We call this the *factorized* fixed point. The corresponding assignment of the full variables is

$$a_i = 0 \quad \forall \langle i, j \rangle \quad b_i = \frac{1}{1 - z^2} \quad \forall \langle i, j \rangle \quad (39)$$

With this solution, we have $\partial_{\bar{z}} b_i = 0$ for all i so that, from (30), the spectral density is $\nu(z) = 0$. Wherever the above solution is stable, the cavity method yields a

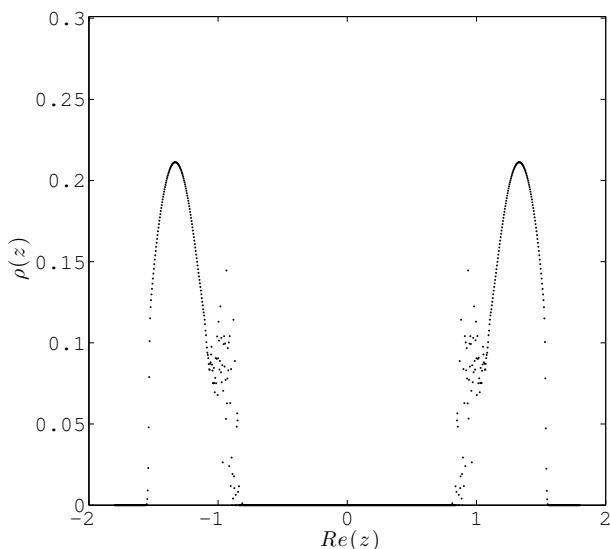


Fig. 3: Slice of the spectral density along the line $\text{Im}(z) = 0.8$: average over 500 different random graphs with 10000 nodes, and were generated with an average degree of $c = 3$. Comparison with figure 2b shows that the location of the peaks inside the circle depends on the instance.

spectral density equal to 0. We will therefore refer to this region as the paramagnetic phase. To study the stability of this solution, we linearize the belief propagation equations (23)-(24) around it. Writing $a_{i \rightarrow j} = 0 + \alpha_{i \rightarrow j}^0$, $b_{i \rightarrow j} = -1/z^2 + \beta_{i \rightarrow j}^0$ where $\alpha_{i \rightarrow j}^0 \in \mathbb{R}$, $\beta_{i \rightarrow j}^0 \in \mathbb{C}$ are the initial infinitesimal perturbations, the evolution of these perturbations when iterating the BP equations is given by the system

$$\alpha_{i \rightarrow j}^{t+1} = \frac{1}{|z|^2} \sum_{l \in \partial i \setminus j} \alpha_{l \rightarrow i}^t, \quad (40)$$

$$\beta_{i \rightarrow j}^{t+1} = \frac{1}{z^2} \sum_{l \in \partial i \setminus j} \beta_{l \rightarrow i}^t. \quad (41)$$

One can rewrite this system in a matrix form using the non-backtracking operator B . It was already remarked in [3], although in a completely different setting, that B arises from the linearization of belief propagation around a factorized fixed point. The linear relations then reads

$$\underline{\alpha}^{t+1} = \frac{1}{|z|^2} B^T \underline{\alpha}^t \quad (42)$$

$$\underline{\beta}^{t+1} = \frac{1}{z^2} B^T \underline{\beta}^t \quad (43)$$

where $\underline{\alpha}, \underline{\beta}$ are two vectors of size $2M$, M being the number of edges of the graph. From these equations we see that the paramagnetic solution is stable if and only if the largest eigenvalue of B (in absolute value) is smaller than $|z|^2$. Therefore the bulk is constrained to the disk

$$|z| \leq \sqrt{\rho(B)} \quad (44)$$

where we have introduced the spectral radius $\rho(B)$ of the non-backtracking operator. Instability of the factorized belief propagation fixed point signals a phase transition in the associated particle system.

The above result is valid for any graph where the cavity method applies. We expect this to encompass at least all locally tree-like ensembles. Eq. (44) supports the heuristic used [3] on real networks to consider as informative only the eigenvalues that lie outside of the circle of radius $\sqrt{\rho(B)}$. For an Erdős-Rényi graph $\rho(B) = c$.

The existence of a factorized fixed point, and hence of a paramagnetic phase in which the spectral density is exactly 0, seems to be a special feature of the non-backtracking matrix. For instance, one can compute the spectral density for the (symmetric) adjacency matrix A , see e.g. [8]. The Hamiltonian is then again quadratic, and couples N Gaussian variables x_i . The marginals of the x_i are again completely determined by their (complex) variance Δ_i , as is the spectral density which is proportional to the average of $\text{Im}\Delta_i$ over the graph. Using the same notations as before, the BP equations read [8]

$$\Delta_{i \rightarrow j}(z) = \left(z - \sum_{l \in \partial i \setminus j} \Delta_{l \rightarrow i}(z) \right)^{-1} \quad (45)$$

for which no factorized (site-independent) solution exists. The spectral density of the adjacency matrix instead exhibits Lifshitz tails [2] that spoil the gap between the bulk and the eigenvalues reminiscent of the presence of clusters. Similar results hold for the other matrices commonly used for spectral clustering.

Numerical results. – We solve the belief propagation equations on a single graph. For a given point $z \in \mathbb{C}$ in the complex plane, we iterate (23)-(24) and (31)-(33) until convergence, and output the spectral density as given by (30)¹. BP is found to always converge to a real-valued spectral density.

Figure 1a shows the results of BP for a typical random graph of size 10000, with average degree $c = 3$. We expect this figure to be a fairly close approximation of the thermodynamic limit. For comparison, figure 1b shows the spectral density as computed by histogramming the eigenvalues of many matrices. The discrepancies between the two figures are of two types. The first one consists of the tails that extend beyond the black circle in the direct diagonalization case. These represent sub-extensive contributions to the spectral density as can be seen from figure 2, that disappear in the thermodynamic limit, in agreement with the prediction from BP. The second type of discrepancy consist of the tails inside the circle in figure 1b that are absent from figure 1a. As can be seen from 2b,

¹Another approach, aiming at computing the spectral density in the thermodynamic limit is the population dynamics algorithm which we also implemented. It, however, suffered from lack of convergence, symptomized by a non-vanishing imaginary part of the spectral density.

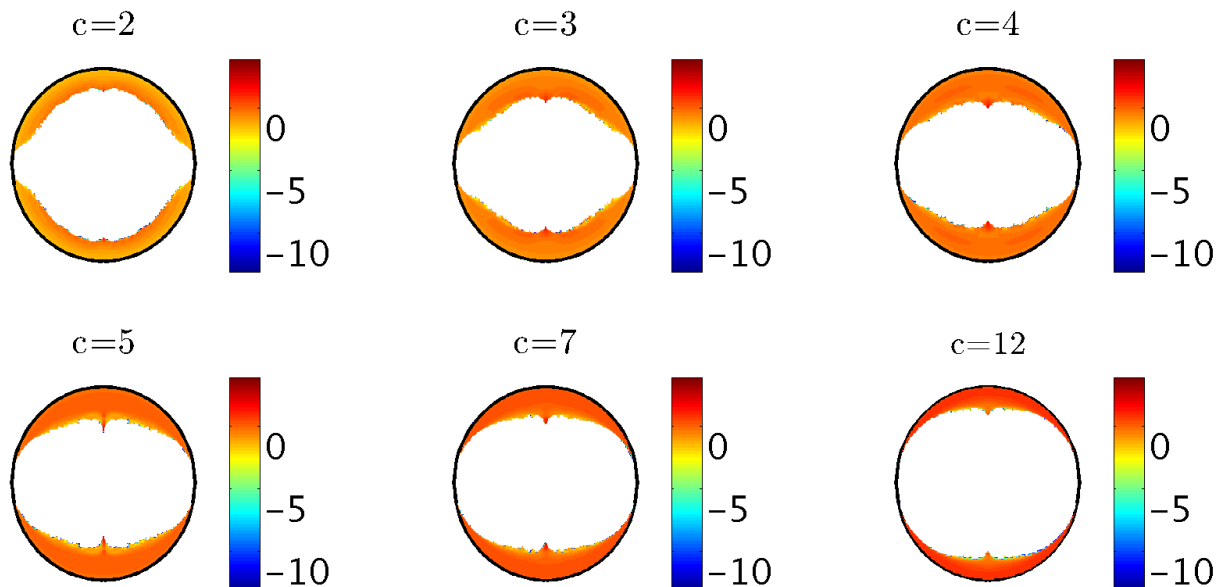


Fig. 4: Spectral density for different average degrees in $\ln z$ -scale. The support becomes closer and closer to the circle with bigger c , as expected because of the exact computation in the regular case.

these tails do not seem to vanish in the large N limit. As supported by figure 3, they seem to originate from very localized peaks in the spectral density, that BP fails to see because of the finite resolution of the grid used. Finally, we show in figure 4 the spectral density computed by BP for 6 different values of the average degree. As shown in [3], in the regular case, the spectral density is non-zero only on the circle of radius $\sqrt{d} - 1$. For an Erdős-Rényi graph, in the large degree limit, we expect the spectral density to be non-zero only in a region close to the circle of radius \sqrt{c} , because for a Poissonian graph, the excess degree is also Poissonian of mean c .

Conclusion. – The study of the spectral density of the non-backtracking operator in the thermodynamic limit by means of the cavity method allows to understand better its remarkable efficiency to perform spectral clustering. A phase transition-like behavior at the boundary of the circle provides a physical insight on why its spectral density vanishes sharply instead of exhibiting Lifshitz tails, like other popular choices of spectral methods. Additionally, the non-backtracking operator seems to have puzzling properties still unexplained, like the ability to predict the number of clusters in a graph from counting real eigenvalues outside of the circle of radius $\sqrt{\rho(B)}$. This fact will be investigated in future work.

This work has been supported by the ERC under the European Union's 7th Framework Programme Grant Agreement 307087-SPARCS.

REFERENCES

- [1] VON LUXBURG U., *Statistics and computing*, **17** (2007) 395.
- [2] KHORUNZHIY O., KIRSCH W., MÜLLER P. *et al.*, *The Annals of Applied Probability*, **16** (2006) 295.
- [3] KRZAKALA F., MOORE C., MOSSEL E., NEEMAN J., SLY A., ZDEBOROVÁ L. and ZHANG P., *Proceedings of the National Academy of Sciences*, **110** (2013) 20935.
- [4] EDWARDS S. and JONES R. C., *Journal of Physics A: Mathematical and General*, **9** (1976) 1595.
- [5] RODGERS G. and BRAY A., *Physical Review B*, **37** (1988) 3557.
- [6] SEMERJIAN G. and CUGLIANDOLO L. F., *Journal of Physics A: Mathematical and General*, **35** (2002) 4837.
- [7] KÜHN R., *Journal of Physics A: Mathematical and Theoretical*, **41** (2008) 295002.
- [8] ROGERS T., CASTILLO I. P., KÜHN R. and TAKEDA K., *Physical Review E*, **78** (2008) 031116.
- [9] ROGERS T. and CASTILLO I. P., *Phys. Rev. E*, **79** (2009) 012101.
- [10] NERI I. and METZ F., *Physical review letters*, **109** (2012) 030602.
- [11] MEZARD M. and MONTANARI A., *Information, physics, and computation* (Oxford University Press) 2009.
- [12] HASHIMOTO K.-i., *Automorphic forms and geometry of arithmetic varieties.*, (1989) 211.
- [13] BASS H., *International Journal of Mathematics*, **3** (1992) 717.
- [14] ANGEL O., FRIEDMAN J. and HOORY S., *arXiv preprint arXiv:0712.0192*, (2007) .
- [15] DECELLE A., KRZAKALA F., MOORE C. and ZDEBOROVÁ L., *Physical Review E*, **84** (2011) 066106.
- [16] MASSOULIE L., *arXiv preprint arXiv:1311.3085*, (2013) .
- [17] MOSSEL E., NEEMAN J. and SLY A., *arXiv preprint arXiv:1311.4115*, (2013) .